AMERICAN SOCIETY FOR MICROBIOLOGY | mBio®

RESEARCH ARTICLE

Ligand-Mediated Biofilm Formation via Enhanced Physical Interaction between a Diguanylate Cyclase and Its Receptor

David Giacalone,[a] T. Jarrod Smith,[a] Alan J. Collins,[a] Holger Sondermann,[c] Lori J. Koziol,[b] George A. O'Toole[a]

[a]Department of Microbiology and Immunology, Geisel School of Medicine at Dartmouth, Hanover, New Hampshire, USA

[b]Department of Biology, New England College, Henniker, New Hampshire, USA

[c]Department of Molecular Medicine, College of Veterinary Medicine, Cornell University, Ithaca, New York, USA

ABSTRACT The bacterial intracellular second messenger, cyclic dimeric GMP (c-di-GMP), regulates biofilm formation for many bacteria. The binding of c-di-GMP by the inner membrane protein LapD controls biofilm formation, and the LapD receptor is central to a complex network of c-di-GMP-mediated biofilm formation. In this study, we examine how c-di-GMP signaling specificity by a diguanylate cyclase (DGC), GcbC, is achieved via interactions with the LapD receptor and by small ligand sensing via GcbC's calcium channel chemotaxis (CACHE) domain. We provide evidence that biofilm formation is stimulated by the environmentally relevant organic acid citrate (and a related compound, isocitrate) in a GcbC-dependent manner through enhanced GcbC-LapD interaction, which results in increased LapA localization to the cell surface. Furthermore, GcbC shows little ability to synthesize c-di-GMP in isolation. However, when LapD is present, GcbC activity is significantly enhanced (~8-fold), indicating that engaging the LapD receptor stimulates the activity of this DGC; citrate-enhanced GcbC-LapD interaction further stimulates c-di-GMP synthesis. We propose that the I-site of GcbC serves two roles beyond allosteric control of this enzyme: promoting GcbC-LapD interaction and stabilizing the active conformation of GcbC in the GcbC-LapD complex. Finally, given that LapD can interact with a dozen different DGCs of *Pseudomonas fluorescens*, many of which have ligand-binding domains, the ligand-mediated enhanced signaling via LapD-GcbC interaction described here is likely a conserved mechanism of signaling in this network. Consistent with this idea, we identify a second example of ligand-mediated enhancement of DGC-LapD interaction that promotes biofilm formation.

IMPORTANCE In many bacteria, dozens of enzymes produce the dinucleotide signal c-di-GMP; however, it is unclear how undesired cross talk is mitigated in the context of this soluble signal and how c-di-GMP signaling is regulated by environmental inputs. We demonstrate that GcbC, a DGC, shows little ability to synthesize c-di-GMP in the absence of its cognate receptor LapD; GcbC-LapD interaction enhances c-di-GMP synthesis by GcbC, likely mediated by the I-site of GcbC. We further show evidence for a ligand-mediated mechanism of signaling specificity via increased physical interaction of a DGC with its cognate receptor. We envision a scenario wherein a "cloud" of weakly active DGCs can increase their activity by specific interaction with their receptor in response to appropriate environmental signals, concomitantly boosting c-di-GMP production, ligand-specific signaling, and biofilm formation.

KEYWORDS CACHE domain, *Pseudomonas fluorescens*, biofilm, c-di-GMP, receptor, signaling

Received 7 June 2018 **Accepted** 18 June 2018 **Published** 10 July 2018

Citation Giacalone D, Smith TJ, Collins AJ, Sondermann H, Koziol LJ, O'Toole GA. 2018. Ligand-mediated biofilm formation via enhanced physical interaction between a diguanylate cyclase and its receptor. mBio 9:e01254-18. https://doi.org/10.1128/mBio.01254-18.

Editor Joanna B. Goldberg, Emory University School of Medicine

Address correspondence to George A. O'Toole, georgeo@Dartmouth.edu.

This article is a direct contribution from a Fellow of the American Academy of Microbiology. Solicited external reviewers: Matt Parsek, University of Washington; Urs Jenal, Biozentrum/University of Basel.

For most bacteria, biofilm formation is a highly regulated event (1, 2). The bacterial intracellular second messenger, cyclic dimeric GMP (c-di-GMP), controls biofilm formation by regulating a diversity of biofilm-relevant outputs (3), including flagellar motility (4), extracellular polysaccharide production (5, 6), adhesin localization (7), and transcriptional control of pathways important for early biofilm formation (8). An important research theme in the field has been understanding the mechanism(s) of c-di-GMP signaling specificity in the context of microbes that can have >50 proteins that make, degrade, and bind this second messenger.

Biofilm formation by *Pseudomonas fluorescens* Pf0-1 occurs when the adhesin LapA localizes to the cell surface (9). LapA is maintained on the cell surface when the inner membrane protein LapD binds c-di-GMP. The c-di-GMP-bound, inner membrane-localized LapD sequesters LapG; thus, this protease is unable to target the N-terminal cleavage site of LapA (10, 11). One example of how c-di-GMP is specifically transferred to the LapD receptor is by physical interaction with a diguanylate cyclase (DGC) (12). The DGC called GcbC has been shown to physically interact with LapD utilizing a surface-exposed α-helix of the GGDEF domain on GcbC and a surface-exposed α-helix of the EAL domain of LapD (12). We also demonstrated previously that the I-site of GcbC contributes to the interaction of this enzyme with LapD (13). This direct interaction model was proposed as one means to confer signaling specificity (12, 14).

GcbC is an inner membrane protein that contains a putative calcium channel chemotaxis receptor (CACHE) domain N terminal to its GGDEF domain; this CACHE domain is predicted to reside in the periplasm. CACHE domains can be responsible for small ligand sensing (15). Many signal transduction proteins, including DGCs and histidine kinases, contain CACHE domains, which are involved in modulating these enzyme activities (16–18). GcbC, along with five other DGCs encoded on the *P. fluorescens* Pf0-1 genome (Pfl01_1336, Pfl01_2295, Pfl01_2297, Pfl01_3550, and Pfl01_3800), contain putative periplasmic CACHE domains located N-terminally to their GGDEF domain, suggesting that these six DGCs are capable of sensing and responding to small ligands. The predicted domain organization of three of these CACHE-containing proteins, GcbC, Pfl01_2295, and Pfl01_2297, is shown in Fig. 1A.

In this study, we analyze the putative CACHE domain of GcbC and identify two environmentally relevant organic acids, including citrate, as a ligand for this DGC. We show citrate-enhanced physical interaction of GcbC and LapD and that this enhanced interaction promotes increased c-di-GMP synthesis by GcbC, thereby promoting biofilm formation. We also describe another example of such ligand-mediated enhancement of biofilm formation, suggesting the generality of this mechanism. Furthermore, we show that GcbC has little propensity to synthesize c-di-GMP in isolation; it is only in the presence of its receptor, LapD, that GcbC makes high levels of c-di-GMP. We propose that the I-site of GcbC serves two roles beyond allosteric control of this enzyme: promoting LapD-GcbC interaction and stabilizing the active conformation of GcbC in this complex. Thus, we propose a mechanism whereby GcbC engagement with its receptor LapD, which is enhanced by environmental cues, could serve as a general mechanism to confer specificity to this complex signaling network.

RESULTS

Citrate-mediated biofilm enhancement is dependent on GcbC activity. Automated domain annotation software predicts a CACHE domain in the periplasmic portion of GcbC (Fig. 1A). To identify small molecules that the CACHE domain of GcbC may bind, we performed a CLUSTAL alignment of this amino acid sequence with CACHE domains of known structure (19). GcbC showed the highest amino acid similarity to rpHK1S-Z16 (PDB accession no. or identifier [ID] 3LIF) of *Rhodopseudomonas palustris* with 31% identity (see Fig. S1 in the supplemental material). When crystallized, the CACHE domain of rpHK1S-Z16 was bound to citrate and methyl-2,4-pentanediol, two small ligands recruited from the crystallization cocktail (19). Because ligand binding by CACHE domains has been shown to activate the C-terminally fused histidine kinase (HK)

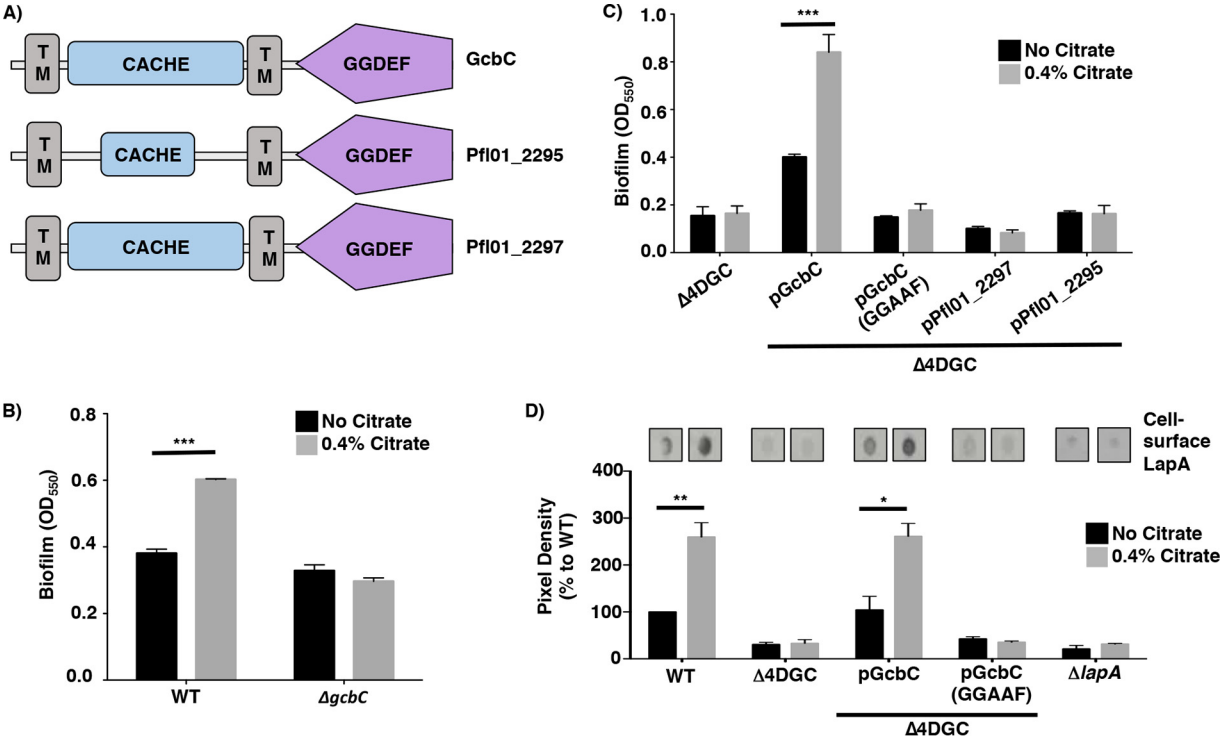

FIG 1 Citrate stimulates biofilm formation via GcbC. (A) Predicted domain organization of GcbC, Pfl01_2295, and Pfl01_2297 as predicted by SMART (33). The domains are indicated in each block (TM, transmembrane domain). Analysis of Pfl01_2295 using the MiST2 database (34) predicts a second transmembrane domain. (B) Biofilm formation by WT *P. fluorescens* and the Δ*gcbC* mutant in the presence and absence of 0.4% citrate. Mean values plus standard deviations (SDs) (error bars) are shown ($n = 3$). (C) Biofilm formation by the indicated strains in the presence and absence of citrate. In this panel, the Δ4DGC mutant background is used, with the WT GcbC and the catalytically inactive variant (GGAAF) introduced into this mutant on plasmids. Pfl01_2297 and Pfl01_2295 are two other CACHE-domain-containing diguanylate cyclases in *P. fluorescens*, expressed from the same vector backbone, that serve as controls. (D) Quantification of cell surface levels of LapA in the presence and absence of 0.4% citrate. Representative blots are shown. For panels B, C, and D, the values shown are averages for three replicates (plus SDs). Values that are significantly different from the value for the strain grown without citrate by Student's *t* test are indicated by a horizontal black bar and asterisks as follows: *, *P* value of <0.05; **, *P* value of <0.01; ***, *P* value of <0.001.

and DGC domains (17, 18), we hypothesized that citrate may stimulate GcbC activity to enhance biofilm formation.

To test this idea, we compared the impact of citrate on biofilm formation in the wild-type (WT) *P. fluorescens* Pf0-1 and a *gcbC* mutant. In a WT background, a 50% increase in biofilm formation was observed in the presence of citrate (Fig. 1B). However, citrate-mediated enhancement of biofilm formation observed for the WT strain was abolished in the *gcbC* mutant (Fig. 1B), suggesting that citrate-mediated enhancement of biofilm formation is dependent on the presence of GcbC. Also, we found that increasing concentrations of citrate further enhanced biofilm formation of *P. fluorescens* by up to ~100% (Fig. S2A).

Next, we selected the CACHE domain-containing Pfl01_2295 and Pfl01_2297 proteins (Fig. 1A), both of which interact with LapD (20), to serve as controls to determine whether other CACHE domains also respond to citrate to promote biofilm formation. For these studies, we used a *P. fluorescens* Pf0-1 strain lacking four DGCs, referred to as Δ4DGC, which does not form a biofilm under our laboratory conditions; this low c-di-GMP-producing strain was previously used to investigate c-di-GMP production by other *P. fluorescens* DGCs (21). The four DGCs deleted in the Δ4DGC strain, identified previously, are encoded by the *gcbA*, *gcbB*, *gcbC*, and *wspR* genes (21). Of the three CACHE domain-containing DGCs expressed in the Δ4DGC mutant background (GcbC, Pfl01_2295, and Pfl01_2297), only the strain expressing GcbC responded to citrate with increased biofilm formation (Fig. 1C). DGC-mediated c-di-GMP synthesis typically requires an intact GGDEF active site motif, and mutation of this motif to GGAAF in GcbC eliminates catalytic activity; this GcbC (GGAAF) mutant variant was shown previously to

be stably expressed at a level equivalent to the WT protein (21). When the GcbC-GGAAF mutant protein was expressed in the Δ4DGC mutant background, biofilm formation was abolished, and notably, citrate-mediated biofilm formation was also abolished (Fig. 1C).

We further assessed the functionality of GcbC, Pfl01_2295, and Pfl01_2297 as active DGCs via assaying their ability to stimulate increased production of the Pel polysaccharide using Congo red (CR) binding assay. Increased CR binding indicates increased production of the Pel polysaccharide, which is mediated by increased c-di-GMP production; thus, dark red colonies indicate robust Pel production, and white colonies indicate a lack of Pel production. Each DGC was cloned into an expression plasmid, then electroporated into *Pseudomonas aeruginosa* PA14 and grown under inducing conditions with 0.1% arabinose. When GcbC and Pfl01_2295 are expressed from a plasmid, CR binding of Pel polysaccharide was robustly stimulated compared to the vector-only control (pMQ72 [Fig. S3]). When Pfl01_2297 was expressed from a plasmid, CR binding of Pel polysaccharide was, at best, weakly stimulated compared to the vector-only control. As a control, a mutant defective in production of the Pel polysaccharide (Δ*pelA*) showed little CR binding (Fig. S3). These data indicate that Pfl01_2295 and Pfl01_2297 are likely functional DGCs, a point addressed further below.

Importantly, citrate-enhanced biofilm formation is dependent on LapA (Fig. S2B), indicating that citrate acts via the known LapD-LapG-LapA pathway. To further support a role for LapA in citrate-stimulated biofilm formation, we used *P. fluorescens* Pf0-1 strains carrying a hemagglutinin (HA)-tagged LapA variant to detect the amount of LapA at the cell surface, as reported previously (7, 10), as a function of the presence of citrate. In a WT *P. fluorescens* strain, citrate caused a 159% increase in LapA pixel density, which suggests a higher abundance of LapA at the cell surface in the presence of citrate (Fig. 1D). Only when GcbC was present and catalytically active did citrate cause an increase in cell surface-associated LapA (Fig. 1D). As a control, minimal levels of signal were detected in a *P. fluorescens* strain lacking LapA, as expected. Also, there were no detected differences in the amount of LapA in whole-cell lysate in the presence and absence of citrate in WT *P. fluorescens* (Fig. S2C). Taken together, these data show that citrate-mediated stimulation of biofilm formation by WT *P. fluorescens* Pf0-1 requires the active diguanylate cyclase GcbC and is associated with enhanced cell surface LapA.

Citrate also enhances the growth of *P. fluorescens* (Fig. S2D), but as described below, this enhanced growth is not the basis for the enhanced biofilm formation in the presence of citrate. Interestingly, despite its ability to stimulate biofilm formation, citrate caused an ~100% increase in swimming motility (Fig. S2E), perhaps via the ability of citrate to enhance growth of *P. fluorescens*.

The putative ligand-binding site of the CACHE domain is important for GcbC-mediated biofilm formation. CACHE domains are ubiquitous, periplasmic, ligand-binding domains (15, 16). In a previous study, the RXYF motif was found to be the most conserved feature among the characterized CACHE domains (19). A mutation of the RXYF motif of the CACHE domain of KinD, a histidine kinase in *Bacillus subtilis*, caused this microbe to lose its ability to respond to root exudates, and resulted in decreased biofilm formation on tomato roots compared to a WT strain (17).

We first assessed whether citrate-enhanced biofilm formation was due to increased protein expression level. We measured protein levels of a HA-tagged GcbC variant (expressed from a plasmid from the studies shown in Fig. 1C and D) in the presence and absence of citrate and found that citrate did not affect the production and/or stability of GcbC (Fig. 2A). Analysis of the pixel density of the bands in the presence and absence of citrate revealed a ratio of 1.05 $\pm$ 0.08, indicating no change in GcbC protein level when the cells are grown with citrate.

We next sought to identify the putative site where citrate might bind to GcbC using the known structures of CACHE domains (Fig. 2B, left; template PDB ID 3LIB). As in the other CACHE domains, the tyrosine residue of the RXYF motif of GcbC was predicted to point toward the ligand-binding site (Fig. 2B and Fig. S4). Furthermore, based on the CACHE domain model of GcbC, the amino acids R139, R162, and R172 were identified

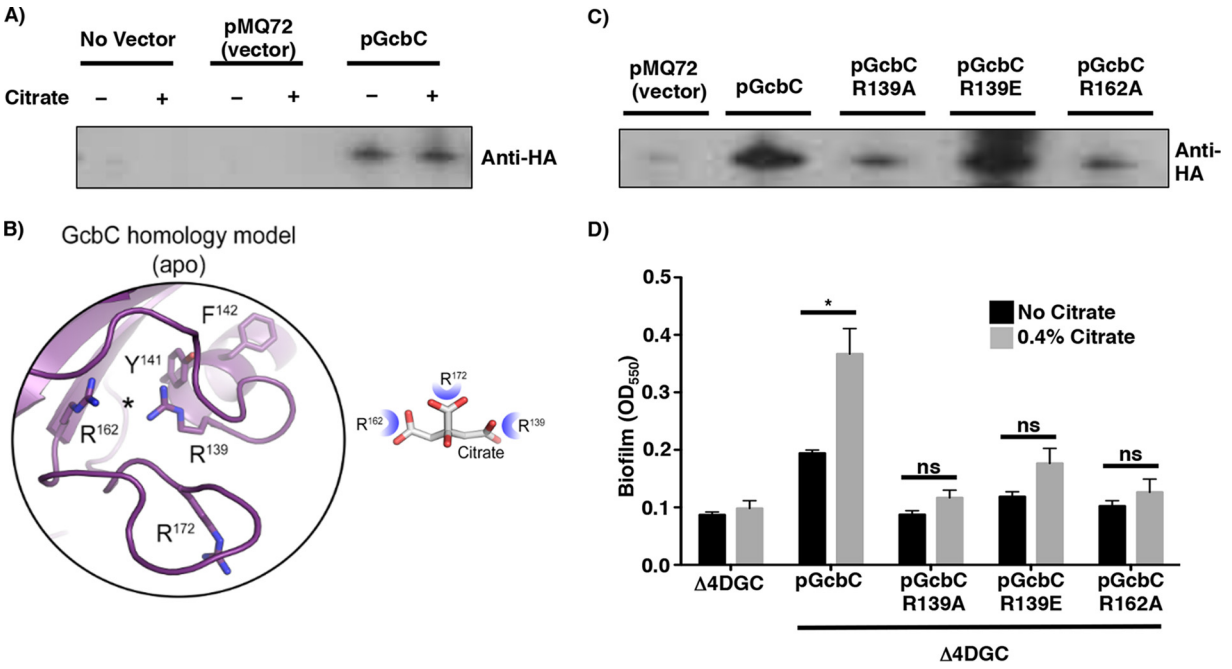

FIG 2 Effects of CACHE domain mutations on biofilm formation. (A) Western blot to assess the level of hemagglutinin-tagged GcbC (GcbC-HA) expressed from a plasmid in the presence (+) and absence (−) of citrate. This is the GcbC-HA-expressing plasmid used in Fig. 1. (B) Homology model of the CACHE domain of GcbC based on rpHK1S-Z16 (PDB ID 3LIF) and vpHK1S-Z8 (PDB ID 3LID) (see Fig. S1 and S4 in the supplemental material) to identify the putative ligand-binding site. (C) Western blot assessment of the relative stability of GcbC-R139A-HA, GcbC-R139E-HA and GcbC-R162A-HA mutant proteins compared to the WT GcbC. These proteins were all expressed in Δ4DGC mutant *P. fluorescens* strain. (D) Quantitative analysis of biofilm formation by strains expressing the indicated CACHE domain mutants in the presence and absence of citrate. Values shown are the averages plus SDs for three replicates. Values that are significantly different ($P < 0.05$) for the strain grown without citrate and with citrate by Student's *t* test are indicated by a black horizontal bar and asterisk. Values that are not significantly different (ns) are indicated.

as candidates to shape the predicted ligand-binding site (Fig. 2B, right). On the basis of the model, we predict that three arginine residues can coordinate the three carboxylic acid groups of citrate (Fig. 2B, right). R139 is also part of the RXYF motif. To probe whether these residues were involved in the citrate-mediated enhancement of biofilm formation, each of the arginine residues forming the putative ligand-binding site was mutated in GcbC and the mutant protein expressed from a plasmid introduced into the Δ4DGC mutant background. Mutating R172 (R172A and R172E) resulted in loss of stability of GcbC (see Table S1 in the supplemental material); however, GcbC-R139A, GcbC-R139E, and GcbC-R162A variants were detected by Western blotting, with GcbC-R139E variant present at approximately WT levels (Fig. 2C).

We next assessed whether the CACHE domain was required for citrate-enhanced biofilm formation. The strain carrying GcbC-R139E variant, as well as the less stable GcbC-R139A and GcbC-R162A alleles, did not show a significant enhancement of biofilm formation in the presence of citrate (Fig. 2D). We further expanded our search for important conserved residues within the CACHE domain that were predicted based on alignments with other CACHE domain proteins; however, the other 27 mutant proteins we constructed were unstable (Table S1). Together, our data indicate that the RXYF motif, and specifically R139 of the putative citrate-binding arginine triad, is critical for GcbC-dependent, citrate-mediated enhancement of biofilm formation.

Selected organic acids stimulate biofilm formation via GcbC. We next sought to identify other ligands that may be sensed by the CACHE domain of GcbC, given that some characterized CACHE domains bind multiple ligands (19, 22). On the basis of the ability of the putative arginine triad to bind the three carboxyl groups of citrate, we tested whether other organic acids (Fig. S5A), including acetate (C_2), pyruvate (C_3), succinate (C_4), fumarate (C_4), α-ketoglutarate (C_5), or isocitrate (C_6) could enhance biofilm formation in a GcbC-dependent manner. In both a WT *P. fluorescens* strain and

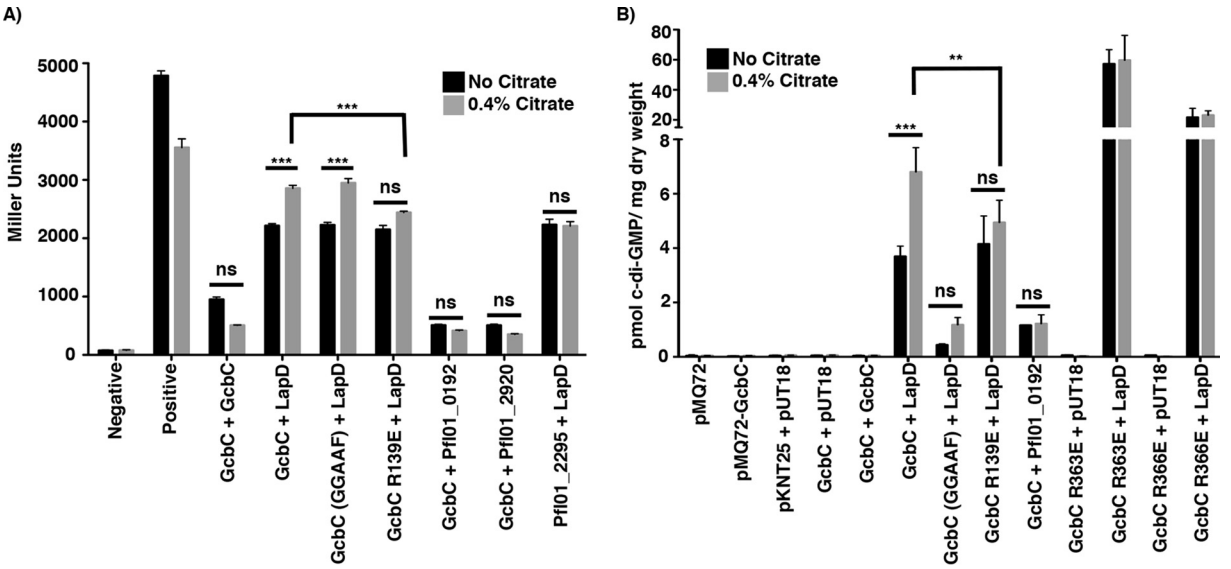

FIG 3 Citrate-mediated biofilm enhancement. (A) The effect of citrate on interaction with the indicated proteins is compared by the B2H assay and expressed in Miller units. Pfl01_2295 is a DGC containing a CACHE domain, Pfl01_0192 is a protein containing GGDEF and EAL domains, and Pfl01_2920 is a protein containing an EAL domain. Briefly, the proteins of interest fused to two halves of the catalytic domain of an adenylate cyclase from *Bordetella pertussis* (T25 and T18) are transformed into *E. coli* BTH101 cells (32). Plasmids pKNT25 and pUT18 are the vector-only controls. If the two proteins interact, the adenylate cyclase activity is reconstituted, promoting cyclic AMP (cAMP) synthesis, which in turn activates transcription of the *lacZ* gene and increases production of its gene product. β-Galactosidase activity (shown in Miller units on the *y* axis) is assessed using *ortho*-nitrophenyl-β-galactoside (ONPG) as a substrate, which serves as a measure of the degree of interaction (32). Citrate did not enhance interaction of the vectors or of the positive control (GCN4 leucine zipper protein) (Positive). Citrate enhanced only the interaction between LapD and GcbC. The effect of catalytic activity of GcbC on interaction with LapD was compared in the presence and absence of 0.4% citrate. Mutation of the putative citrate-binding pocket in the CACHE domain of GcbC (GcbC-R139E) resulted in the loss of citrate-stimulated GcbC-LapD interaction. (B) The B2H assay strains were used to measure the effects of citrate on c-di-GMP synthesis by GcbC. Plasmids were cotransformed as indicated into *E. coli* BTH101. After 24 h of incubation at 30°C, nucleotides were extracted. c-di-GMP production in *E. coli* BTH101 was determined for strains producing the indicated proteins. Only coexpression of LapD and GcbC showed appreciable accumulation of c-di-GMP, which was significantly stimulated by added citrate. For panels A and B, all experiments were performed in triplicate, and values are means plus SDs (error bars). Values that are significantly different for each strain grown with and without citrate by Student's *t* test are indicated by asterisks as follows: **, *P* value of $<$0.01; ***, *P* value of $<$0.001. Values that are not significantly different (ns) are indicated. For panel B, GcbC-LapD and GcbC R139E-LapD interactions are represented by six biological replicates instead of three.

when GcbC is expressed in a Δ4DGC mutant strain, only isocitrate significantly enhanced biofilm formation, and did so by 40% (Fig. S5B). Like citrate, isocitrate is a C_6 compound which contains three carboxyl groups (Fig. S5A). Also, isocitrate did not stimulate biofilm formation by the strain carrying the GcbC-R139E variant (Fig. S5C), indicating that the R139E variant was not responsive to citrate or isocitrate. Taken together, these data indicate that the CACHE domain of GcbC likely binds citrate and isocitrate.

Citrate-mediated interaction of GcbC with LapD enhances synthesis of c-di-GMP. In our published model, GcbC mediates biofilm formation by transferring c-di-GMP to LapD through physical interaction, as demonstrated by both pulldown and bacterial two-hybrid assay (12). We further showed that the LapD-GcbC interaction is mediated via the $\alpha5^{GGDEF}$ helix of GcbC with the $\alpha2^{EAL}$ helix of LapD (12). This LapD-GcbC interaction also requires the I-site of GcbC (13). We asked whether citrate might exert its effect of stimulating biofilm formation via stabilization of the LapD-GcbC signaling complex. To test whether citrate bolsters GcbC-LapD interaction, we exploited the bacterial two-hybrid system used to initially demonstrate interaction between these proteins (12). We did observe a modest but significant enhancement of LapD-GcbC interaction in the presence of citrate (Fig. 3A). No such enhancement was observed for the control interactions: LapD-Pfl01_2295, or GcbC with a dual-domain protein (Pfl01_0192; this protein has cytoplasmic GGDEF and EAL domains similar to LapD) or a phosphodiesterase (Pfl01_2920) (Fig. 3A). Citrate also did not enhance GcbC-GcbC dimerization (Fig. 3A). Further, the catalytically inactive variant of GcbC still showed citrate-stimulated interaction similar to WT GcbC (Fig. 3A). Finally, the GcbC-R139E

mutant variant did not show a significant, citrate-mediated increased interaction (Fig. 3A), consistent with our data above that this residue is required for citrate-mediated enhancement of biofilm formation (Fig. 2D).

We further explored whether citrate could also enhance the diguanylate cyclase activity of GcbC. We used the bacterial two-hybrid (B2H) plasmids and strains to express GcbC and LapD outside of their native context and to better focus on how the interaction of these two proteins might specifically impact GcbC's activity. The activity of GcbC was assessed by measuring the level of c-di-GMP extracted from the *Escherichia coli* strains that carry plasmids containing the indicated genes (Fig. 3B). The level of c-di-GMP measured in the *E. coli* strain carrying the vector control was $<$0.5 pmol c-di-GMP/mg (dry weight) of bacteria (Fig. 3B). This low background level of c-di-GMP provided a useful tool to measure differences in c-di-GMP levels derived from GcbC in the presence and absence of citrate and the LapD receptor.

GcbC alone did not synthesize c-di-GMP above the background level, and citrate did not promote c-di-GMP production using three different strains wherein only GcbC was expressed (Fig. 3B; pMQ72-GcbC, pKNT25-GcbC plus pUT18, and pKNT25-GcbC plus pUT18-GcbC), a finding consistent with a previous study in which low levels of c-di-GMP synthesis by GcbC were detected (21). Coexpression of GcbC with LapD resulted in ~4 pmol c-di-GMP/mg (dry weight), an ~8-fold increase above the control level, and the level of c-di-GMP was further significantly increased to ~7 pmol c-di-GMP/mg (dry weight) upon the addition of citrate (Fig. 3B). This finding has two important implications. First, GcbC activity is apparently stimulated when engaging its cognate LapD receptor, suggesting a mechanism for specific signaling between GcbC and LapD. Second, enhanced interaction of GcbC and LapD upon the addition of citrate further enhances c-di-GMP production by GcbC.

Modest amounts of c-di-GMP catalysis occurred when the catalytically inactive GcbC variant was coexpressed with LapD, but the addition of citrate did not significantly enhance the level of c-di-GMP (Fig. 3B). Additionally, Pfl01_0192, a dual GGDEF-EAL domain protein with a cytoplasmic domain organization similar to LapD, which was shown to interact weakly with GcbC (Fig. 3A), produced c-di-GMP in the presence of GcbC at levels that were above the background level but did not increase with added citrate (Fig. 3B).

We investigated the impact of the GcbC-R139E CACHE domain mutation on citrate-mediated LapD-GcbC interaction and c-di-GMP synthesis. While the GcbC-R139E–LapD interaction was equivalent to the interaction between LapD and the wild-type GcbC, citrate-enhanced interaction of GcbC-R139E–LapD showed a small, but nonsignificant, increase (Fig. 3A). This finding was consistent with the data above (Fig. 2D), showing that the GcbC-R139E mutant was still capable of promoting biofilm formation in the Δ4DGC background, but biofilm formation was not enhanced by the addition of citrate. Furthermore, and consistent with the bacterial two-hybrid data, basal c-di-GMP levels were not affected by the GcbC-R139E mutant variant compared to the WT GcbC when coexpressed with LapD (Fig. 3B). Importantly, there was no significant increase in c-di-GMP level when the GcbC-R139E mutant variant was coexpressed with LapD in the presence of citrate (Fig. 3B). Thus, our data indicate that LapD-GcbC interaction enhances c-di-GMP production, and the addition of citrate stimulates both interaction of LapD-GcbC and c-di-GMP synthesis, likely via the CACHE domain of GcbC.

When GcbC is removed from its native context and expressed in a heterogenous system, this enzyme did not produce c-di-GMP above the background level (Fig. 3B). This finding suggested that GcbC might be inactive until it engages its cognate receptor, LapD. To test this idea, we assessed c-di-GMP production by I-site mutant variants of this enzyme expressed in the B2H *E. coli* strain. The canonical role of the I-site is to reduce GcbC catalytic activity when c-di-GMP is bound, and we previously identified two different mutations of GcbC near the I-site, R363E and R366E, which greatly enhanced biofilm formation and c-di-GMP levels when expressed in *P. fluorescens* (13). These I-site-proximal mutations also reduced interaction with LapD (13). When expressed on its own, the GcbC-R366E I-site mutant was not able to synthesize

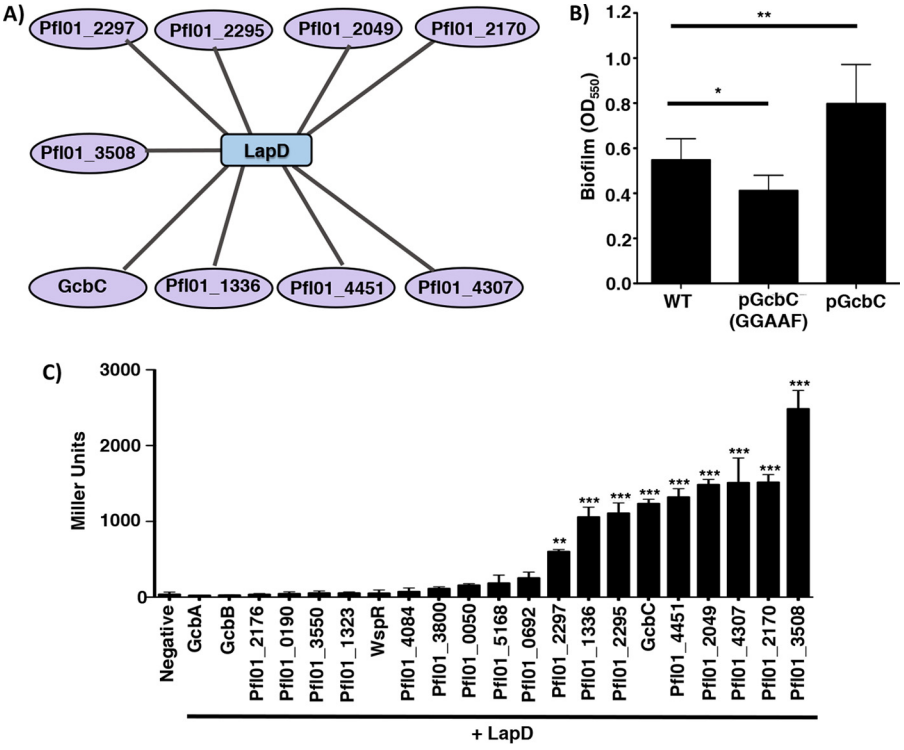

FIG 4 LapD interacts with multiple DGCs. (A) Interaction map of DGCs that showed a significant level of interaction with LapD by 24 h compared to the negative control by B2H assay. Data that served as the basis for this model are shown in panel C. (B) Biofilm formation of WT *P. fluorescens*. WT GcbC and the catalytically inactive variant (GGAAF) were expressed on plasmids. Experiments were performed in triplicate (values are means plus SDs), with an indicated *P* value of either <0.05 (*) or <0.01 (**) by a Student's *t* test comparing each strain to WT *P. fluorescens*. (C) Plasmids containing each of the 21 DGCs and LapD were cotransformed into *E. coli* BTH101. After 24 h of incubation at 30°C, cells were scraped from the plate, and β-galactosidase levels were measured to identify LapD interaction partners. Of the 21 DGCs tested, 9 were identified as significantly interacting with LapD by B2H assay compared to the vector-only (negative) control. Pfl01_2297, Pfl01_1336, Pfl01_2295, GcbC, Pfl01_4451, Pfl01_2049, Pfl01_4307, Pfl01_2170, and Pfl01_3508 significantly interacted with LapD, but the level of interaction with LapD varied among the nine DGCs. Assays were performed in triplicate with two biological replicates (means plus SDs are shown). Statistical significance was evaluated by a one-way analysis of variance (ANOVA) analysis followed by a Tukey multiple comparison analysis test, comparing the value for each DGC-LapD interaction to the value for the negative control. Asterisks indicate a *P* value of either <0.01 (**) or <0.001 (***).

c-di-GMP above the background level (Fig. 3B). We observe a similar phenotype for the R363E mutant; R363 stabilizes the GGDEF domains as they come together in a GGDEF dimer with c-di-GMP at the I-site. Only when LapD was present were high levels of c-di-GMP produced, with the GcbC-R363E-expressing strain synthesizing ~60 pmol c-di-GMP/mg (dry weight) and the GcbC-R366E-expressing strain synthesizing ~20 pmol c-di-GMP/mg (dry weight) (Fig. 3B). These levels of c-di-GMP were significantly higher than the level detected for wild-type GcbC, and citrate did not further enhance c-di-GMP production for either I-site mutant (Fig. 3B). These data strongly support the model that GcbC has little or no activity until this enzyme engages its cognate receptor.

A conserved mechanism of signaling specificity. We next explored whether the mechanism we defined for GcbC-LapD interactions might apply to any of the other 20 DGCs in *P. fluorescens*. We found that LapD is a central hub of DGC interaction; LapD interacts with nine different DGCs in a pairwise bacterial two-hybrid assay (Fig. 4A and C). Included among the nine DGCs that interact with LapD are the CACHE domain-containing DGCs Pfl01_2295 and Pfl01_2297, and the putative SadC homolog, Pfl01_4451 (Fig. 4A). SadC is a DGC identified for its role in the early stages of biofilm formation by *P. aeruginosa* (6, 23), and the Δ*sadC* mutant of *P. aeruginosa* shows an

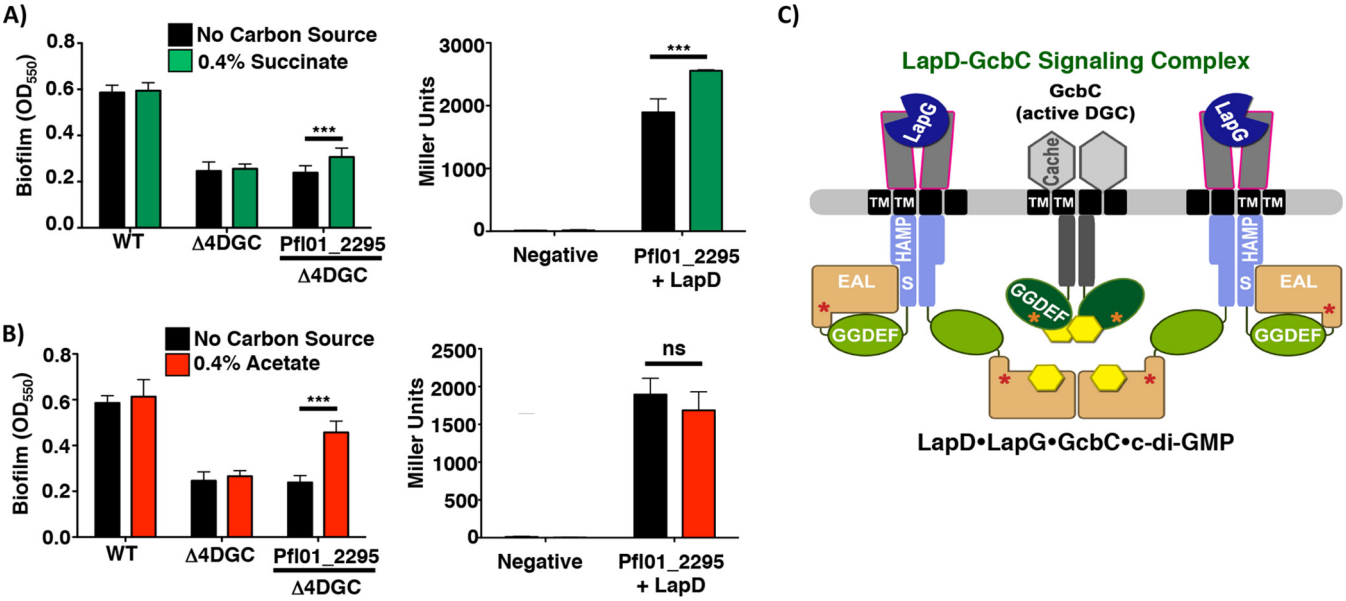

FIG 5 Identification of potential ligands sensed by Pfl01_2295. The results of biofilm assays and B2H assays with the indicated strains and proteins are shown. For each panel, the presence and absence of each organic acid was compared for both biofilm assay and B2H assay. (A and B) Strains were grown in the presence and absence of succinate (A) and acetate (B). Biofilm assay data are from six biological replicates (means plus SDs). B2H assays were performed in triplicate (means plus SDs). Linear models implemented in R (35) were used to identify organic acid-supplemented media whose properties significantly differed from the base medium for both biofilm assay (K10T-1 minimal medium [see Materials and Methods]) and B2H assay experiments. *P* values of <0.05 were considered significant. **, $P < 0.01$; ***, $P < 0.001$. (C) A model of a GcbC, LapD, and LapG "basket" signaling complex (24). In this model, the DGC- and PDE-like domains are indicated by the GGDEF and EAL residues typically associated with the active enzymes; we showed previously that these domains of LapD are not active. Instead, the PDE-like domain of LapD binds c-di-GMP (yellow hexagon). The GGDEF domain of GcbC functions as an active DGC in this context. The HAMP signal transduction domain and the S helix of LapD, the CACHE domain of GcbC, the transmembrane (TM) domains, I-sites (red and orange stars), and the LapG periplasmic protease are also indicated.

approximately 50% reduction of global, cellular c-di-GMP levels compared to WT *P. aeruginosa* PA14 (23).

Given that there are nine DGCs that interact with LapD, we hypothesized that each of the nine DGCs may compete with one another to interact with LapD. To test this model, we overexpressed WT GcbC and the catalytically inactive variant of GcbC in a WT *P. fluorescens* strain. When the catalytically inactive GcbC variant was overexpressed, biofilm formation was significantly reduced by ~20% (Fig. 4B), indicating that the catalytically inactive variant of GcbC is displaying a dominant-negative phenotype, a finding consistent with our competition hypothesis. As a control, when WT GcbC was overexpressed, biofilm formation was significantly enhanced, as expected (Fig. 4B).

We next explored whether the ligand-mediated signaling specificity mechanism is conserved among other CACHE-containing DGCs. We focused on Pfl01_2295, as this DGC shows levels of interaction with LapD similar to those observed for GcbC (Fig. 4C), and the likely robust c-di-GMP synthesis activity as indicated by the robust CR binding observed when Pfl01_2295 was expressed from a plasmid in *P. aeruginosa* (Fig. S3). Also, the CACHE domain of Pfl01_2295 contains the conserved RXYF motif (Fig. S6), and contains two of the three arginine residues that comprise the putative ligand-binding site of the CACHE domain of GcbC. Thus, we predicted that Pfl01_2295 would sense ligands that are similar to, but different from, citrate. To test this idea, we expressed Pfl01_2295 in the Δ4DGC mutant background and performed a biofilm assay with medium supplemented with exogenous acetate, pyruvate, succinate, fumarate, or isocitrate. Citrate was shown not to stimulate biofilm formation through Pfl01_2295 nor enhance LapD-Pfl01_2295 interaction as measured using the bacterial two-hybrid assay (Fig. 1C and 3A).

Succinate significantly enhanced biofilm formation in the presence of Pfl01_2295 and also significantly enhanced interaction with LapD (Fig. 5A). Thus, this finding mirrored what we observed for citrate and isocitrate with GcbC. Interestingly, acetate

significantly stimulated Pfl01_2295-dependent biofilm formation but did not stimulate interaction with LapD (Fig. 5B), perhaps indicating that acetate stimulates Pfl01_2295 activity but not the ability of this DGC to interact with its receptor. Pyruvate, fumarate, and isocitrate had no effect in stimulating biofilm formation in a Δ4DGC mutant background with Pfl01_2295 expressed from a plasmid (Fig. S7).

DISCUSSION

A key open question relating to c-di-GMP signaling is how specificity of a particular output can be mediated in the context of up to dozens of enzymes or receptors making, breaking, and binding this dinucleotide second messenger. Here, our data suggest two related mechanisms for controlling output specificity. First, GcbC shows little activity unless it is coexpressed with its receptor. Furthermore, we show that an extracellular ligand can modulate the activity of a GcbC and does so via promoting interaction of the DGC with its cognate receptor. Our data are consistent with the model that citrate or isocitrate binding to the CACHE domain of GcbC enhances interaction with LapD. We propose that the increased interaction between GcbC and LapD has two important consequences: stabilization of a complex that allows direct transfer of the GcbC-generated c-di-GMP signal to the LapD receptor, and equally importantly, activation of the DGC activity of GcbC. Our data suggest that for at least this DGC, GcbC must be in a complex with its receptor to be activated. An additional boost in cyclic nucleotide production was measured when citrate or isocitrate was added to the medium in a strain coexpressing GcbC and LapD, indicating that the enhanced GcbC-LapD interaction also enhanced DGC activity. Furthermore, recent work from the Sondermann lab (24) identified a LapD dimer of dimers as a c-di-GMP- and LapG-bound state, which could serve as an interaction platform or "receptor basket" for GcbC, thereby forming a large LapD–LapG–GcbC– c-di-GMP signaling complex (Fig. 5C). Our data add to this model a ligand-based mechanism to enhance the interaction between GcbC and LapD, and thus signaling specificity in the context of a large signaling network.

We suggest a possible mechanism whereby c-di-GMP production by GcbC is promoted when this DGC is in complex with LapD. Our data here suggest that as a baseline condition, GcbC activity is low, a finding consistent with a previous study in which low levels of c-di-GMP synthesis by GcbC were detected (21). Surprisingly, we detected little c-di-GMP production by two different I-site-proximal variants of GcbC when this enzyme was expressed on its own, consistent with the idea that this enzyme is likely inactive when not engaging its receptor. How then does the GcbC-LapD interaction stimulate GcbC activity? We reported previously the somewhat unexpected finding that the I-site of GcbC is required for full LapD-GcbC interaction (13). Partly on the basis of this finding, we propose that the I-site of this diguanylate cyclase (Fig. 5C, orange stars in GcbC) may engage LapD (rather than c-di-GMP) to help promote stabilization of the active form of the GcbC. In this model, we propose that it is only when local c-di-GMP levels become very high that GcbC is driven toward the inactive state via I-site binding by the dinucleotide. The addition of citrate may further stabilize the active conformation of GcbC, both by enhancing GcbC-LapD interaction via the GcbC I-site (and likely other interactions [13]) and promoting higher levels of c-di-GMP production.

We have identified two C_6, three-carboxyl-group-containing organic acids, citrate and isocitrate, as potential ligands that bind to GcbC via its CACHE domain. There are an abundance of CACHE domains present as components of signal transduction proteins (16), including proteins involved in c-di-GMP signaling, and yet, the role of CACHE domains in regulating DGC activity is poorly understood. Our data show that citrate and isocitrate are likely ligands for the CACHE domain associated with GcbC. *P. fluorescens*, a plant growth-promoting microbe, forms biofilms on tomato roots; root exudates contain high levels of low-molecular-weight organic acids, including citrate (25–27). We suggest that many compounds found in root exudates, including additional organic acids, sugars, and metals, may be used as signals by *P. fluorescens* to promote biofilm formation.

As we have shown here, GcbC appears to sense citrate and isocitrate, but not a variety of other structurally related molecules. It is possible that the CACHE domain of GcbC responds to additional signals. For example, in *Pseudomonas syringae* pv. *actinidiae*, the CACHE domain PscD (PDB ID 5G4Z) binds glycolate, acetate, propionate, and pyruvate (22), indicating that CACHE domains allow for some promiscuity in their binding of ligands. GcbC has been shown to be part of a large signaling network, interacting with a phosphodiesterase and multiple dual-domain-containing proteins (20), thus also providing the possibility that different ligands sensed via the CACHE domain of GcbC could dictate which proteins interact with this DGC.

We showed that while GcbC responds to exogenous citrate and isocitrate, other CACHE domain-containing DGCs do not respond to these organic acids. We identified the RXYF motif as important for signal sensing by GcbC. Furthermore, the R162 residue, but not R172, is conserved among the CACHE domains of GcbC, Pfl01_2295, Pfl01_2297, and Pfl01_3800 (see Fig. S6 in the supplemental material); thus, this variation in sequence likely speaks to the inability of these other DGCs to respond to the same ligands as GcbC. Consistent with the idea that these other CACHE domains bind other signals, we have identified acetate and succinate as potential ligands that are sensed via the CACHE domain of Pfl01_2295. Only succinate enhanced Pfl01_2295-LapD interaction, while acetate promoted Pfl01_2295-dependent biofilm formation but did not enhance LapD interaction. Thus, ligand binding may exert a variety of effects on target proteins. Such a finding may not be surprising in the context of this complex c-di-GMP network, as multiple pathways contribute to biofilm formation, and many DGCs have multiple interaction partners (20). Additional work is required to identify all of the ligands that impact the c-di-GMP network in this organism.

Together, our data indicate that extracellular ligands, via their ability to impact protein-protein interactions and/or DGC activity, can modulate c-di-GMP signaling specificity. We think it is unlikely that all nine DGCs shown to interact with LapD do so simultaneously and with high affinity. Rather, we envision a scenario wherein a "cloud" of DGCs with low activity perhaps weakly interact with their receptor(s); a specific DGC-receptor interaction may increase in response to appropriate environmental signals, concomitantly boosting c-di-GMP production, ligand-specific signaling, and biofilm formation. Overall, our work provides insight into a ligand-mediated mechanism conferring signaling specificity within a complex network of enzymes and receptors that make, break, and bind c-di-GMP. Given the large number of ligand-binding domains associated with c-di-GMP-metabolizing proteins, the data presented here could represent a general means of regulating c-di-GMP-controlled outputs by enhancing specific interactions between c-di-GMP-metabolizing enzymes and their effectors.

MATERIALS AND METHODS

Strains and media. Bacterial strains used in this study are listed in Table S2 in the supplemental material, and were cultured and maintained in lysogeny broth (LB) or on 1.5% agar LB plates. *Pseudomonas fluorescens* was grown at 30°C, and *Pseudomonas aeruginosa* and *Escherichia coli* was grown at 37°C. *E. coli* S17-1-λ-pir was used for maintenance and transfer of plasmids. *Saccharomyces cerevisiae* strain InvSc1 was used for plasmid modification as described previously (28, 29). K10T-1 medium was prepared as described previously (30). Sodium citrate was added to 1.5% agar LB plates and K10T-1 medium to a final concentration of 13.6 mM (0.4% [wt/vol]) for all the experiments described. All organic acids were set at 0.4% (wt/vol), and the following concentrations were used: sodium acetate (29.4 mM), pyruvic acid (45.4 mM), sodium succinate (14.8 mM), sodium fumarate (25.0 mM), α-ketoglutarate (27.4 mM), and isocitrate (15.5 mM). The following antibiotics were used as indicated: gentamicin (15 μg/ml for *E. coli*, 30 μg/ml for *P. fluorescens* and *P. aeruginosa*), kanamycin (50 μg/ml for *E. coli*), and carbenicillin (50 μg/ml for *E. coli*).

Biofilm assay. Biofilm assays were performed as described previously (1). *P. fluorescens* Pf0-1 strains were incubated in K10T-1 minimal medium with and without 0.4% organic acid, as indicated, for 6 h at 30°C. Biofilms were stained with 0.1% crystal violet, washed with water, and then solubilized with a solution consisting of 45% methanol, 45% distilled water (dH_2O), and 10% glacial acetic acid. The optical density (OD) of the solubilized crystal violet solution was measured at 550 nm to determine the amount of biofilm formed.

Dot blot for LapA localization assay. Localization of LapA to the cell surface was measured using a hemagglutinin (HA)-tagged LapA variant integrated into the chromosome of *P. fluorescens* as described previously with slight modifications (7, 10, 31). Bacterial cultures were grown overnight in LB and then

subcultured into 5 ml of K10T-1 medium at a 1:50 dilution for 6 h at 30°C. To test how sodium citrate affected LapA localization to the cell surface, sodium citrate was added at the beginning of the 6-h subculturing period. After 6 h of incubation, cells were normalized to the lowest OD value and washed twice in K10T-1 medium, and 5-μl aliquots were spotted onto a nitrocellulose membrane. Once dried, HA-tagged LapA was probed for by Western blot analysis.

Bacterial two-hybrid assay. Bacterial two-hybrid (B2H) assays were performed using *E. coli* BTH101 cells based on a previously described system (32). Briefly, ~100 ng of each bacterial two-hybrid plasmid was cotransformed into *E. coli* BTH101 by electroporation. *E. coli* BTH101 cells were incubated on LB agar supplemented with 50 μg/ml kanamycin, 50 μg/ml carbenicillin, and 0.5 mM isopropyl-β-D-1-thiogalactopyranoside (IPTG) for 24 h at 30°C. At 24 h, either β-galactosidase or c-di-GMP levels were quantified as described below. β-Galactosidase assays were performed as exactly described previously (12) to quantify the extent of protein-protein interaction. β-Galactosidase levels are presented in Miller units.

c-di-GMP quantification assay. c-di-GMP was extracted from *E. coli* BTH101 cells after incubation on LB agar plates at 30°C for 24 h. The cells were scraped from the plate surface with 1 ml of dH_2O, then pelleted, and resuspended in 0.250 ml nucleotide extraction buffer (40% methanol, 40% acetonitrile, 20% dH_2O, and 0.1 N formic acid), followed by incubation at −20°C for 1 h. The cells were pelleted again, and the reaction was neutralized by transfer of 0.2 ml nucleotide extract to 8 μl of 15% NH_4CO_3. Nucleotide extracts were vacuum dried and resuspended in 0.2 ml high-performance liquid chromatography (HPLC)-grade H_2O. c-di-GMP concentration was analyzed by liquid chromatography-mass spectrometry and compared to a standard curve of known c-di-GMP concentration, as reported previously (12). The moles of c-di-GMP were normalized to the dry weight of the cell pellet from which the nucleotides were extracted.

Congo red binding assay. Assessment of DGC activity using the Congo red binding assays was performed as described previously (12).

Swim motility assay. Swim motility assays were performed as described previously (21). K10T-1 plates containing 0.35% agar were prepared by adding filter-sterilized K10T-1 medium to an autoclaved, molten agar solution, and plates were solidified for 3 h. Overnight cultures were normalized to the lowest OD value and washed twice in K10T-1 medium. A 2- to 200-μl pipette micropipette tip was used to inoculate each plate. A sterile pipette tip was dipped into each strain and plunged halfway into the swim agar plate. The plates were incubated at 30°C for ~30 h, and the plates were photographed. The swim area was calculated using ImageJ software.

Growth curve assay. The amount of growth of *P. fluorescens* in the presence and absence of citrate was measured. Bacterial cultures were grown overnight in liquid LB and then subcultured in 5 ml K10T-1 medium with and without 0.4% citrate at a 1:50 ratio for 6 h at 30°C. Every 2 h, the OD of the bacterial culture was measured at 600 nm to determine the amount of growth that occurred.

SUPPLEMENTAL MATERIAL

Supplemental material for this article may be found at https://doi.org/10.1128/mBio.01254-18.

FIG S1, PDF file, 0.1 MB.
FIG S2, PDF file, 0.2 MB.
FIG S3, PDF file, 0.1 MB.
FIG S4, PDF file, 0.2 MB.
FIG S5, PDF file, 0.1 MB.
FIG S6, PDF file, 0.1 MB.
FIG S7, PDF file, 0.1 MB.
TABLE S1, PDF file, 0.05 MB.
TABLE S2, PDF file, 0.1 MB.

ACKNOWLEDGMENTS

We thank members of the lab for helpful discussions, the reviewers for their helpful comments, and Tom Hampton for assistance with statistical analysis.

This work was supported by the NIH via grant R01GM123609 (to H.S. and G.A.O.) and P20 RR030360.

REFERENCES

1. O'Toole GA, Kolter R. 1998. Initiation of biofilm formation in *Pseudomonas fluorescens* WCS365 proceeds via multiple, convergent signaling pathways: a genetic analysis. Mol Microbiol 28:449–461. https://doi.org/10.1046/j.1365-2958.1998.00797.x.
2. Prüss BM, Besemann C, Denton A, Wolfe AJ. 2006. A complex transcription network controls the early stages of biofilm development by *Escherichia coli*. J Bacteriol 188:3731–3739. https://doi.org/10.1128/JB.01780-05.
3. Römling U, Gomelsky M, Galperin MY. 2005. c-di-GMP: the dawning of a novel bacterial signaling system. Mol Microbiol 57:629–639. https://doi.org/10.1111/j.1365-2958.2005.04697.x.
4. Baker AE, Diepold A, Kuchma SL, Scott JE, Ha DG, Orazi G, Armitage JP, O'Toole GA. 2016. A PilZ domain protein FlgZ mediates cyclic-di-GMP-dependent swarming motility control in *Pseudomonas aeruginosa*. J Bacteriol 198:1837–1846. https://doi.org/10.1128/JB.00196-16.

5. Ross P, Weinhouse H, Aloni Y, Michaeli D, Weinberger-Ohana P, Mayer R, Braun S, de Vroom E, van der Marel GA, van Boom JH, Benziman M. 1987. Regulation of cellulose synthesis in *Acetobacter xylinum* by cyclic diguanylic acid. Nature 325:279–281. https://doi.org/10.1038/325279a0.
6. Merritt JH, Brothers KM, Kuchma SL, O'Toole GA. 2007. SadC reciprocally influences biofilm formation and swarming motility via modulation of exopolysaccharide production and flagellar function. J Bacteriol 189:8154–8164. https://doi.org/10.1128/JB.00585-07.
7. Monds RD, Newell PD, Gross RH, O'Toole GA. 2007. Phosphate-dependent modulation of c-di-GMP levels regulates *Pseudomonas fluorescens* Pf0-1 biofilm formation by controlling secretion of the adhesin LapA. Mol Microbiol 63:656–679. https://doi.org/10.1111/j.1365-2958.2006.05539.x.
8. Martínez-Gil M, Ramos-González MI, Espinosa-Urgel M. 2014. Roles of cyclic di-GMP and the Gac system in transcriptional control of the genes coding for the *Pseudomonas putida* adhesins LapA and LapF. J Bacteriol 196:1484–1495. https://doi.org/10.1128/JB.01287-13.
9. Hinsa SM, Espinosa-Urgel M, Ramos JL, O'Toole GA. 2003. Transition from reversible to irreversible attachment during biofilm formation by *Pseudomonas fluorescens* WCS365 requires an ABC transporter and a large secreted protein. Mol Microbiol 49:905–918. https://doi.org/10.1046/j.1365-2958.2003.03615.x.
10. Newell PD, Monds RD, O'Toole GA. 2009. LapD is a bis-(3′-5′)-cyclic dimeric GMP-binding protein that regulates surface attachment by *Pseudomonas fluorescens* Pf0-1. Proc Natl Acad Sci U S A 106:3461–3466. https://doi.org/10.1073/pnas.0808933106.
11. Navarro MV, Newell PD, Krasteva PV, Chatterjee D, Madden DR, O'Toole GA, Sondermann HA. 2011. Structural basis for c-di-GMP-mediated inside-out signaling controlling periplasmic proteolysis. PLoS Biol 9:e1000588. https://doi.org/10.1371/journal.pbio.1000588.
12. Dahlstrom KM, Giglio KM, Collins AJ, Sondermann H, O'Toole GA. 2015. Contribution of physical interactions to signaling specificity between a diguanylate cyclase and its effector. mBio 6:e01978-15. https://doi.org/10.1128/mBio.01978-15.
13. Dahlstrom KM, Giglio KM, Sondermann H, O'Toole GA. 2016. The inhibitory site of a diguanylate cyclase is a necessary element for interaction and signaling with an effector protein. J Bacteriol 198:1595–1603. https://doi.org/10.1128/JB.00090-16.
14. Dahlstrom KM, O'Toole GA. 2017. A symphony of cyclases: specificity in diguanylate cyclase signaling. Annu Rev Microbiol 71:179–195. https://doi.org/10.1146/annurev-micro-090816-093325.
15. Anantharaman V, Aravind L. 2000. Cache—a signaling domain common to animal Ca^{2+}-channel subunits and a class of prokaryotic chemotaxis receptors. Trends Biochem Sci 25:535–537. https://doi.org/10.1016/S0968-0004(00)01672-8.
16. Upadhyay AA, Fleetwood AD, Adebali O, Finn RD, Zhulin IB. 2016. Cache domains that are homologous to, but different from PAS domains comprise the largest superfamily of extracellular sensors in prokaryotes. PLoS Comput Biol 12:e1004862. https://doi.org/10.1371/journal.pcbi.1004862.
17. Chen Y, Cao S, Chai Y, Clardy J, Kolter R, Guo JH, Losick R. 2012. A *Bacillus subtilis* sensor kinase involved in triggering biofilm formation on the roots of tomato plants. Mol Microbiol 85:418–430. https://doi.org/10.1111/j.1365-2958.2012.08109.x.
18. Mills E, Petersen E, Kulasekara BR, Miller SI. 2015. A direct screen for c-di-GMP modulators reveals a *Salmonella typhimurium* periplasmic L-arginine-sensing pathway. Sci Signal 8:ra57. https://doi.org/10.1126/scisignal.aaa1796.
19. Zhang Z, Hendrickson WA. 2010. Structural characterization of the predominant family of histidine kinase sensor domains. J Mol Biol 400:335–353. https://doi.org/10.1016/j.jmb.2010.04.049.
20. Dahlstrom KM, Collins AJ, Doing G, Taroni JN, Gauvin TJ, Greene CS, Hogan DA, O'Toole GA. 2018. A multimodal strategy used by a large c-di-GMP network. J Bacteriol 200:e00703-17. https://doi.org/10.1128/JB.00703-17.
21. Newell PD, Yoshioka S, Hvorecny KL, Monds RD, O'Toole GA. 2011. Systematic analysis of diguanylate cyclases that promote biofilm formation by *Pseudomonas fluorescens* Pf0-1. J Bacteriol 193:4685–4698. https://doi.org/10.1128/JB.05483-11.
22. Brewster JL, McKellar JL, Finn TJ, Newman J, Peat TS, Gerth ML. 2016. Structural basis for ligand recognition by a Cache chemosensory domain that mediates carboxylate sensing in *Pseudomonas syringae*. Sci Rep 6:35198. https://doi.org/10.1038/srep35198.
23. Merritt JH, Ha DG, Cowles KN, Lu W, Morales DK, Rabinowitz J, Gitai Z, O'Toole GA. 2010. Specific control of *Pseudomonas aeruginosa* surface-associated behaviors by two c-di-GMP diguanylate cyclases. mBio 1:e00183-10. https://doi.org/10.1128/mBio.00183-10.
24. Cooley RB, O'Donnell JP, Sondermann H. 2016. Coincidence detection and bi-directional transmembrane signaling control a bacterial second messenger receptor. Elife 5:e21848. https://doi.org/10.7554/eLife.21848.
25. Haas D, Défago G. 2005. Biological control of soil-borne pathogens by fluorescent pseudomonads. Nat Rev Microbiol 3:307–319. https://doi.org/10.1038/nrmicro1129.
26. Jones DL. 1998. Organic acids in the rhizosphere—a critical review. Plant Soil 205:25–44. https://doi.org/10.1023/A:1004356007312.
27. de Weert S, Vermeiren H, Mulders IH, Kuiper I, Hendrickx N, Bloemberg GV, Vanderleyden J, De Mot R, Lugtenberg BJ. 2002. Flagella-driven chemotaxis towards exudate components is an important trait for tomato root colonization by *Pseudomonas fluorescens*. Mol Plant Microbe Interact 15:1173–1180. https://doi.org/10.1094/MPMI.2002.15.11.1173.
28. Shanks RMA, Caiazza NC, Hinsa SM, Toutain CM, O'Toole GA. 2006. *Saccharomyces cerevisiae*-based molecular tool kit for manipulation of genes from Gram-negative bacteria. Appl Environ Microbiol 72:5027–5036. https://doi.org/10.1128/AEM.00682-06.
29. Bascom-Slack CA, Dawson D. 1998. A physical assay for detection of early meiotic recombination intermediates in *Saccharomyces cerevisiae*. Mol Gen Genet 258:512–520. https://doi.org/10.1007/s004380050762.
30. Monds RD, Newell PD, Schwartzman JA, O'Toole GA. 2006. Conservation of the Pho regulon in *Pseudomonas fluorescens* Pf0-1. Appl Environ Microbiol 72:1910–1924. https://doi.org/10.1128/AEM.72.3.1910-1924.2006.
31. Newell PD, Boyd CD, Sondermann H, O'Toole GA. 2011. A c-di-GMP effector system controls cell adhesion by inside-out signaling and surface protein cleavage. PLoS Biol 9:e1000587. https://doi.org/10.1371/journal.pbio.1000587.
32. Karimova G, Pidoux J, Ullmann A, Ladant D. 1998. A bacterial two-hybrid system based on a reconstituted signal transduction pathway. Proc Natl Acad Sci U S A 95:5752–5756. https://doi.org/10.1073/pnas.95.10.5752.
33. Schultz J, Milpetz F, Bork P, Ponting CP. 1998. SMART, a simple modular architecture research tool: identification of signaling domains. Proc Natl Acad Sci U S A 95:5857–5864. https://doi.org/10.1073/pnas.95.11.5857.
34. Ulrich LE, Zhulin IB. 2010. The MiST2 database: a comprehensive genomics resource on microbial signal transduction. Nucleic Acids Res 38:D401–D407. https://doi.org/10.1093/nar/gkp940.
35. R Core Team. 2016. R: a language and environment for statistical computing. R Foundation for Statistical Computing, Vienna, Austria. https://www.R-project.org/.